^{178,179,180}Hf and ^{180}Ta(n,γ) cross sections and their contribution to stellar nucleosynthesis

H. Beer
Kernforschungszentrum Karlsruhe GmbH, Institut für Angewandte Kernphysik, D-7500 Karlsruhe, Federal Republic of Germany

R. L. Macklin
Oak Ridge National Laboratory, Oak Ridge, Tennessee 37830
(Received 19 May 1982)

The neutron capture cross sections of ^{178,179,180}Hf were measured in the energy range 2.6 keV to 2 MeV. The average capture cross sections were calculated and fitted in terms of strength functions. Resonance parameters for the observed resonances below 10 keV were determined by a shape analysis. Maxwellian averaged capture cross sections were computed for thermal energies kT between 5 and 100 keV. The cross sections for $kT=30$ keV were used to determine the population probability of the 8^- isomeric level in ^{180}Hf by neutron capture as $(1.24\pm0.06)\%$ and the r-process abundance of ^{180}Hf as 0.0290 (Si $\equiv 10^6$). These quantities served to analyze s- and r-process nucleosynthesis of ^{180}Ta.

NUCLEAR REACTIONS ^{178,179,180}Hf(n,γ), $E=2.6-2000$ keV, measured $\sigma(E)$, deduced ^{178,179,180}Hf resonance parameters, strength functions, average level spacings, Maxwellian averaged capture cross sections, analysis of s- and r-process nucleosynthesis of ^{180}Ta.

I. INTRODUCTION

The origin of ^{180}Ta, nature's rarest stable isotope, is one of the puzzles nuclear astrophysicists are confronted with. It is difficult to find a satisfactory nuclear process and astrophysical scenario for this nucleus, normally mentioned in connection with some other odd-odd nuclei, ^{50}V, ^{138}La, and ^{176}Lu, which are also the scope of more or less successful investigations.[1-6]

The discovery of ^{180}Ta dates back only to 1955 (Ref. 7) but then for a long time this rarest isotope was something similar to a white spot in the chart of nuclides because even its most fundamental nuclear properties: spin, parity, and nuclear binding energy, were uncertain.

A further advance in understanding its nucleosynthesis was achieved when the spin and parity were measured to be 9^-.[8] In addition, the question of nuclear binding energy was solved. The surprising result was that the naturally occurring ^{180}Ta is actually an isomeric state[9] with the impressively long half-life of $\geq 3\times10^{14}$ yr.[10] The ground state of ^{180}Ta ($T_{1/2}=8.1$ h) is quickly transmuted into ^{180}W or ^{180}Hf. The 9^- nature of ^{180}Ta^m suggested a neutron capture origin of this nucleus via a small branching mediated by an allowed Gamow-Teller β transition from an 8^- isomeric state in ^{180}Hf.[11] Beer and Ward[11] studied the possibilities of both s- and r-process nucleosynthesis and tried to quantitatively assess their respective contributions to the solar ^{180}Ta^m abundance. This investigation made clear that a variety of quantities must be determined experimentally before further progress could be expected.

In this paper we follow this concept by measuring the neutron capture cross sections of three hafnium isotopes (^{178,179,180}Hf) in the energy range 2.6 keV to 2 MeV. Below 10 keV the resonance structure was resolved and resonance widths and spacings of many individual resonances were obtained. The average isotopic cross sections were described in terms of strength functions, and Maxwellian averaged cross sections were calculated for thermal energies between $kT=5$ and 100 keV. These data allowed us to determine accurately:

(1) the population probability of the 8^- isomeric state in ^{180}Hf by s-process nucleosynthesis and

(2) the r-process abundance of ^{180}Hf which is important for the r-process calculation of ^{180}Ta^m.

In addition, theoretical calculations were carried out to derive a reliable estimate of the ^{180}Ta^m capture cross section from the systematics of the ^{178,179,180}Hf and ^{182,183,184,186}W (Ref. 12) strength functions. Thus this analysis yielded another important piece of information for the *s*-process nucleosynthesis of ^{180}Ta^m.

II. EXPERIMENTAL TECHNIQUE

The measurements were carried out at the Oak Ridge Linear Accelerator (ORELA) in the energy range 2.6 keV to 2 MeV using the time-of-flight technique. The accelerator was operated at a repetition rate of 800 pulses per second with an electron burst width of 15 to 18 ns full width at half maximum. The neutron beam generated was filtered by ^{10}B (0.0269 atoms/b) to eliminate an overlap of slow neutrons. For the high energy runs ($\gtrsim$300 keV) a uranium filter was used in addition. A series of copper collimators in the 40.12 m flight path of the neutrons provided for an approximately 2.6×5.2 cm rectangular beam profile at the sample position. A 0.05 cm thick ^{6}Li glass detector 43 cm in front of the sample was used to monitor the neutron flux.[13] The neutron capture events in the sample were counted via the prompt emitted capture gamma radiation with a pair of fluorocarbon based liquid scintillation detectors symmetrically placed outside the neutron beam at the position of the sample. The Hf samples which consisted of HfO_2 powder plus 10% sulfur binder were pressed to thin 2.6×2.6 cm squares and exposed to the neutron beam in a 6.4 μm thin Mylar foil bag. The amounts and compositions of the samples are summarized in Table I.

In order to derive the total capture cross section from the measurement of the prompt gamma radiation, the recorded capture event must be independent of the details of the gamma-ray cascade. This is achieved by pulse height weighting[14] the observed gamma rays. This procedure results in an efficiency of the C_6F_6 detectors which is proportional to the total energy (binding energy plus kinetic energy) released from the compound nucleus deexcitation. The detection efficiency is then normalized by means of the saturated resonance technique using the 4.9 eV resonance in ^{197}Au.[15] For this purpose a gold sample of 0.0029 atoms/b is placed in the neutron beam.

The capture events are accumulated into 128 pulse height and 18000 time-of-flight channels. For the pulse height a sharp digital threshold is set at 153 keV. Before addition of the events to the stored data the linear pulse of the detector is transmitted to an on-line computer to perform the pulse height weighting.

The time-of-flight data were collected in four different sections with 1, 2, 4, and 8 ns per channel. The energy calibration of the time-of-flight channels was made by well-known resonances in ^{27}Al at 5.903 keV and 1.094 MeV. The pulse height scale is frequently checked with the Compton edge of the 4.43 MeV gamma line of a PuBe source. More details of the experimental technique are found in Refs. 16 and 17.

III. DATA REDUCTION

In a first step the flight time scale is converted to an energy scale. The data are corrected for dead

TABLE I. Sample characteristics.

Weight[a] HfO_2 (g)	Dimensions (cm)	Isotopic fractions[b] (%)				
		^{176}Hf	^{177}Hf	^{178}Hf	^{179}Hf	^{180}Hf
3.988	2.6×2.6×0.14	0.022	1.54	94.72	1.84	1.69
4.746	2.6×2.6×0.16					
4.3785	2.6×2.6×0.15	0.56	3.42	5.42	81.85	8.74
4.3795	2.6×2.6×0.15					
4.394	2.6×2.6×0.15	0.23	1.0	2.22	2.66	93.89
4.395	2.6×2.6×0.15					

[a]These weights include 10% by weight of sulfur which was added as a binder.
[b]The content of ^{174}Hf was $<0.05\%$.

TABLE II. Resonance parameters of resolved s-wave resonances for ^{178,180}Hf.

	E_0 (eV)	Γ_n (eV)	Γ_γ (meV)
	3081	1.16±0.05	51.8±1.7
^{178}Hf	3400	0.94±0.03	52.2±1.5
	6476	2.51±0.10	83.3±3.0
	7497	7.11±0.32	72.6±2.1
			$\bar{\Gamma}_\gamma$=65.0±7.8
	3059	1.29±0.03	47.8±0.9
	3534	1.29±0.06	32.4±1.2
	3676	7.76±0.28	59.6±1.3
	3793	1.57±0.06	39.8±1.2
^{180}Hf	3993	7.84±0.20	76.6±1.2
	4365	9.00±0.28	60.3±1.1
	4477	0.65±0.01	56.8±1.3
	6191	2.10±0.06	63.0±1.4
	6681	1.87±0.04	78.5±1.6
	6977	2.60±0.14	96.5±3.7
			$\bar{\Gamma}_\gamma$=61.1±6.0

time (5−10%), and the time independent (48 counts/s) and accelerator dependent backgrounds are subtracted. The accelerator independent background is determined during each run from the time interval where the ^{10}B filter is nearly black. In addition, it was measured during the periods where the accelerator was off. The accelerator dependent background was obtained from several runs with no sample in the neutron beam and the time independent background substracted. The total background correction at 30 keV amounted to 10−15% corresponding to the individual isotope. Besides these backgrounds there is also a time-dependent, sample dependent background which arises from neutrons scattered in the sample and captured in the structural material of the detection system (fluorine of the scintillator, Al housing of the detectors). Details of this correction and how it is determined can be found elsewhere.[16] For the present isotopes it was below 1.6%. A correction of ~4% is also required for gamma-ray absorption in the Hf samples. The calculation for the present sample-detector geometry for typical average gamma-ray energies showed that it is relatively insensitive to the capture gamma-ray cascade spectrum. In order to get the final cross section for the enriched Hf samples the sulfur and oxygen contribution was taken out. The sample cross sections were corrected to derive the pure isotope cross sections. The minor ^{176}Hf and ^{177}Hf contributions were approximated by ^{178}Hf and ^{179}Hf, respectively.

IV. DATA ANALYSIS

A. Individual resonances

In the energy range between 2.5 and 10 keV the energy resolution (<0.2%) of the measurement is sufficient to resolve individual resonances. Their resonance widths are, in general, found to be narrow compared to our energy resolution. Therefore, only the quantity $g\Gamma_n\Gamma_\gamma/\Gamma$ which is proportional to the resonance area can be extracted. g stands for the statistical spin factor $(2J+1)/[2(2I+1)]$ with compound spin J and target spin I, and Γ_n, Γ_γ, Γ are the neutron, radiative, and total widths of the resonance.

For some resonances Γ is larger than about an eighth of our resolution so that separate values of $g\Gamma_n$ and Γ_γ can be derived with some confidence. The analysis of the resonances was carried out with the computer code LSFIT[18] which provides a least squares fit of the resonances to a sum of Breit-Wigner single or multilevel forms. The program can adjust in one step up to 16 resonances out of an interval of ≤500 channels. It also accounts for resonance self-protection and multiple scattering as well as Doppler and resolution broadening. Resonance energies and $g\Gamma_n\Gamma_\gamma/\Gamma$ or $g\Gamma_n$ and Γ_γ values for the individual isotopes are listed in Tables II−V. Resonances marked with a superscript a are suspected to be multiplets according to an unusually large Γ_γ and/or an asymmetric shape of the reso-

TABLE III. ^{178}Hf(n,γ) resonance capture areas. The stated uncertainty is statistical only.

E_0 (eV)	$\frac{g\Gamma_n\Gamma_\gamma}{\Gamma}$ (meV)	E_0 (eV)	$\frac{g\Gamma_n\Gamma_\gamma}{\Gamma}$ (meV)	E_0 (eV)	$\frac{g\Gamma_n\Gamma_\gamma}{\Gamma}$ (meV)	E_0 (eV)	$\frac{g\Gamma_n\Gamma_\gamma}{\Gamma}$ (meV)
2659	27.6±0.8	4108	18.8±0.8	5424	23.5±1.2	7107	78.9±3.4
2675	10.2±0.5	4134	54.0±1.3	5441	3.3±0.8	7156	74.5±3.5
2720	2.1±0.4	4143	42.8±1.2	5488[a]	103.1±3.0	7225	48.9±1.6
2742	36.8±0.9	4192	8.5±0.9	5543	12.0±1.0	7259	63.7±2.2
2764	1.7±0.5	4201	43.0±1.1	5560	38.2±1.4	7281	53.4±1.6
2772	32.7±0.9	4230	38.2±1.1	5596	6.8±1.0	7362	22.4±1.2
2787	4.0±0.4	4283	7.7±0.7	5684	38.7±1.1	7459	36.6±1.3
2820	5.2±0.5	4310[a]	62.9±2.3	5716	61.7±1.4	7497	71.9±2.1
2836	37.7±0.9	4362	3.3±0.6	5751	48.8±1.2	7550	9.2±1.5
2868	6.2±0.5	4396	10.4±0.7	5775	22.3±1.0	7565	42.1±1.6
2894	28.1±0.9	4417	45.8±1.2	5796	31.8±1.0	7599	17.9±1.3
2963	32.4±0.9	4442	38.5±1.1	5834	60.8±1.3	7615	27.3±1.5
2978	8.7±0.6	4464	7.1±0.8	5882	38.9±1.2	7662	34.2±1.5
3014	9.5±0.6	4476	49.9±1.4	5904	13.2±0.9	7697	70.0±1.8
3025	28.1±0.9	4486	38.2±1.1	5924	9.7±1.7	7752	53.3±1.7
3061	45.1±1.7	4534	6.6±0.6	5934	31.6±1.8	7790	43.4±1.6
3081	49.6±1.5	4550	6.6±0.6	5943	39.4±1.5	7811	25.1±1.4
3116	4.0±0.4	4590	43.3±1.2	5994	9.9±1.0	7835	30.4±1.8
3149	38.6±1.4	4622	37.7±1.2	6043	13.3±1.2	7854	38.6±2.0
3194	7.4±0.4	4635	13.1±0.8	6069	51.3±1.6	7872	25.5±1.8
3207	2.5±0.4	4660	28.9±1.0	6125	5.2±0.9	7890	17.7±1.6
3217	35.8±1.4	4708	8.0±1.1	6145	17.1±1.2	7942	36.1±2.1
3234	3.1±0.4	4714	7.8±0.9	6176	11.5±1.1	7983	44.6±2.0
3261	28.2±0.8	4740	34.7±1.0	6203	38.3±1.5	8014	56.0±2.3
3268	24.0±0.7	4755	10.7±0.7	6266	55.5±1.9	8058	37.7±2.0
3356	2.6±0.4	4789	6.2±0.6	6278	14.2±1.6	8134	41.2±1.9
3366	5.7±0.5	4805	35.6±1.0	6339	45.1±1.6	8188	52.7±2.2
3400	49.4±1.3	4830[a]	14.7±1.1	6362	15.8±1.2	8232	46.7±2.1
3494	36.6±0.9	4864	25.6±1.0	6418	55.8±2.0	8283	26.1±1.7
3503	13.0±0.7	4883	55.4±1.4	6433	47.2±2.0	8338	30.9±1.8
3562	42.8±1.0	4942	11.0±0.7	6476	80.6±2.7	8373	47.5±2.0
3592	12.3±0.6	4970	39.3±1.1	6551	16.2±1.3	8391	24.4±1.9
3612	52.0±1.1	5003	4.6±0.6	6572	13.4±1.2	8431	43.6±1.9
3639	36.9±1.0	5028	49.3±1.3	6618	10.4±1.1	8544	64.2±2.2
3647	3.3±0.6	5071	40.7±1.2	6659[a]	90.7±3.2	8569	36.3±1.8
3722	3.0±0.5	5107	4.9±0.7	6687	36.3±2.0	8605	42.0±2.0
3754	32.3±1.0	5124	31.9±1.1	6715	74.3±3.3	8648	52.7±2.4
3762	9.8±0.8	5159	13.5±1.0	6748	29.3±1.8	8667	54.6±2.5
3769	41.8±1.1	5176	49.9±1.6	6857	38.2±1.9	8715	53.2±2.1
3789	43.5±1.2	5227	52.1±1.6	6878	49.0±2.0	8746	48.2±2.2
3868	18.1±0.8	5245	21.0±1.1	6939[a]	90.9±3.4	8779	61.0±3.2
3895	1.8±0.5	5263	50.1±1.7	6966	13.5±1.7	8796	67.9±2.7
3914	5.9±0.5	5298[a]	81.4±2.4	6984	48.2±2.3	8855	22.1±2.7
3939	36.1±0.9	5342	52.2±1.6	7015[a]	67.4±3.1	8871	45.8±2.3
3990	36.1±1.0	5369	11.5±1.0	7036	15.0±1.7	8899	51.9±2.2
4089	34.2±1.0	5393	41.8±1.5	7054	12.7±1.6	8924	13.0±1.6

[a]Probable doublet or multiplet.

nance. A few illustrations of the fits obtained are shown in Fig. 1.

Most results of resolved resonance parameters reported in the literature for ^{178,179,180}Hf lie below the energy limit of 2.6 keV of our measurements, so that the present results are an extension to higher energies. Only in the case of ^{180}Hf does an overlap with the work of Moxon[19] occur. The resonances

TABLE IV. ^{179}Hf resonance capture areas. The stated uncertainty is statistical only.

E_0 (eV)	$\frac{g\Gamma_n\Gamma_\gamma}{\Gamma}$ (meV)
2660	29.6±1.3
2670	31.2±1.2
2680	28.7±1.0
2698	49.3±1.5
2705	14.3±1.0
2717	20.3±1.0
2725	57.0±2.1
2735	6.7±0.9
2742	31.9±1.2
2749	20.3±1.0
2756	14.4±0.9
2763	28.8±0.9
2775	18.7±0.9
2785	64.8±2.3
2795	64.6±2.3
2808	22.3±1.3
2823	52.7±2.4
2831	23.2±1.0
2838	24.8±0.9
2854	62.5±2.4
2871	10.1±0.7
2879	30.1±1.0
2888	30.1±1.1
2896	51.8±2.5
2906	26.3±1.0
2921	36.2±3.0
2926	24.2±1.8
2933	15.0±1.2
2940	26.3±1.5
2947	17.7±1.5
2955	26.5±1.4
2966	16.1±1.2
2979	48.5±2.7
2984	48.1±2.5
2996	69.8±2.5
3010	12.3±1.3
3021	68.3±2.6
3032	42.4±2.5
3047	51.6±2.3
3062	20.2±1.5
3069	46.9±2.4

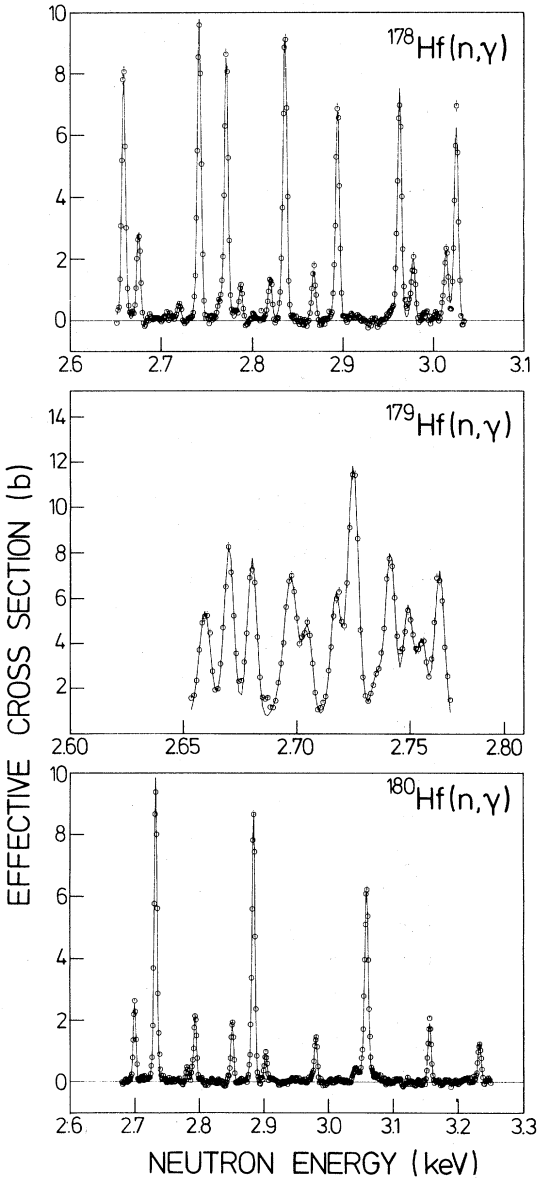

FIG. 1. Samples of ^{178,179,180}Hf(n,γ) yield data. The solid line is generated from the least squares fitting program LSFIT (Ref. 18) to extract resonance parameters. The fit is performed including Doppler broadening, resonance self-protection, multiple scattering, and both Gaussian and exponential resolution functions.

are, however, not well enough resolved to be compared with the present results.

B. Average capture cross sections

For the determination of the effective ^{178,179,180}Hf cross sections in the whole energy region from 2.6 keV to 2 MeV the sample yield data were averaged in $\geq$250 eV bins. This procedure smears out individual resonance fluctuations because more than ten resonances are combined and represents an adequate basis for a parametrization of the cross section in terms of strength functions. The computer code[20] for this analysis which is based on the formalism developed by Dresner[21] adjusts s-, p-, and d-wave

TABLE V. ^{180}Hf(n,γ) resonance capture areas. The stated uncertainty is statistical only.

E_0 (eV)	$\frac{g\Gamma_n\Gamma_\gamma}{\Gamma}$ (meV)	E_0 (eV)	$\frac{g\Gamma_n\Gamma_\gamma}{\Gamma}$ (meV)	E_0 (eV)	$\frac{g\Gamma_n\Gamma_\gamma}{\Gamma}$ (meV)
2700	9.6±0.3	4874	7.9±0.5	7185	11.6±1.2
2733	39.4±0.4	4936	6.9±0.4	7343	36.5±1.5
2782	1.5±0.2	5030	44.1±0.8	7404	58.6±1.9
2794	8.9±0.3	5049	6.5±0.4	7425	12.2±1.3
2851	7.9±0.3	5118	35.8±0.7	7463	43.4±1.6
2884	38.3±0.4	5152	37.3±0.7	7520	24.8±1.3
2903	3.9±0.2	5197	5.4±0.4	7598	7.7±0.7
2981	6.5±0.3	5257	37.3±0.7	7637	47.4±1.1
3042	2.0±0.2	5298	6.3±0.5	7680	22.0±0.9
3059	46.1±0.8	5469	41.8±0.8	7699	13.3±0.8
3156	9.7±0.3	5510	9.2±0.8	7735	50.5±1.1
3233	6.7±0.3	5522	25.8±0.7	7772	14.9±0.8
3275	74.7±0.2	5541	43.2±0.8	7849	20.2±0.8
3307	48.9±0.6	5589	17.6±0.5	7947	22.2±0.9
3385	63.1±0.7	5612	18.7±0.5	7978	22.1±0.9
3534	31.6±1.1	5672	13.6±0.5	8025	49.3±1.3
3571	2.7±0.3	5732	2.5±0.4	8131	42.1±1.1
3583	5.3±0.4	5792	30.7±0.7	8171	5.6±0.8
3613	4.6±0.4	5811[a]	53.0±1.4	8210	36.2±1.1
3649	5.9±0.4	5873	37.3±0.8	8236	44.3±1.2
3661	0.3±0.4	5966	7.8±0.6	8289	10.3±1.0
3676	59.1±1.3	6031	31.6±0.8	8316	40.4±1.3
3706	3.4±0.4	6085	16.0±0.7	8375	9.5±1.0
3780	9.6±0.5	6191	61.2±1.3	8418	6.5±1.0
3793	38.8±1.1	6228	10.3±0.6	8464	15.9±1.2
3879	22.8±0.5	6258	23.3±0.7	8483	8.0±1.3
3972	15.7±0.5	6321	19.8±0.7	8560	47.7±1.5
3993	75.8±1.2	6352	13.0±0.6	8690	93.0±2.6
4038	11.0±0.4	6380	54.9±0.9	8758	19.1±1.3
4064	31.1±0.6	6491	15.4±0.7	8786	13.7±1.2
4143	3.2±0.3	6538	26.4±0.8	8814	35.9±1.4
4190	5.0±0.4	6571	13.0±0.7	8846	14.1±1.1
4253	1.3±0.3	6610	29.6±0.8	8988	43.0±1.5
4286	7.2±0.4	6681	75.3±1.4	9017	17.3±1.2
4322	6.1±0.4	6728	10.4±0.7	9074	59.5±1.7
4365	59.9±1.1	6820	63.6±1.7	9183	6.4±1.0
4477	52.2±1.0	6867	15.0±1.2	9256	49.4±1.4
4530	2.2±0.3	6893	4.6±1.0	9371	53.4±1.5
4591	39.2±1.0	6918	17.6±1.3	9474[a]	86.0±2.7
4600	37.3±0.7	6950[a]	52.2±2.7	9502	45.6±1.6
4681	48.2±0.7	6977	93.0±3.3	9647	44.3±1.6
4764	19.7±0.5	7050	60.3±1.8	9707	57.1±1.7
4810	55.1±0.8	7073	14.3±1.2	9792	9.5±1.1
4828	22.9±0.6	7123	43.9±1.5	9837	50.1±1.7
4862	16.0±0.5	7146	56.0±1.7	9865	22.5±1.3

[a]Probable doublet or multiplet.

strength functions for the elastic scattering channel whereas the capture channel is accounted for with a single average radiation strength. The calculation also includes the correction of self-protection and multiple scattering in the sample. These are opposing effects which both decrease over the measured energy range. The combined correction factor ranges from 0.89 at 2.9 keV, to 1.07 at 440 keV, and to 1.01 at 2 MeV. The individual isotope correction terms at 30 keV are 0.048—0.051 for multiple

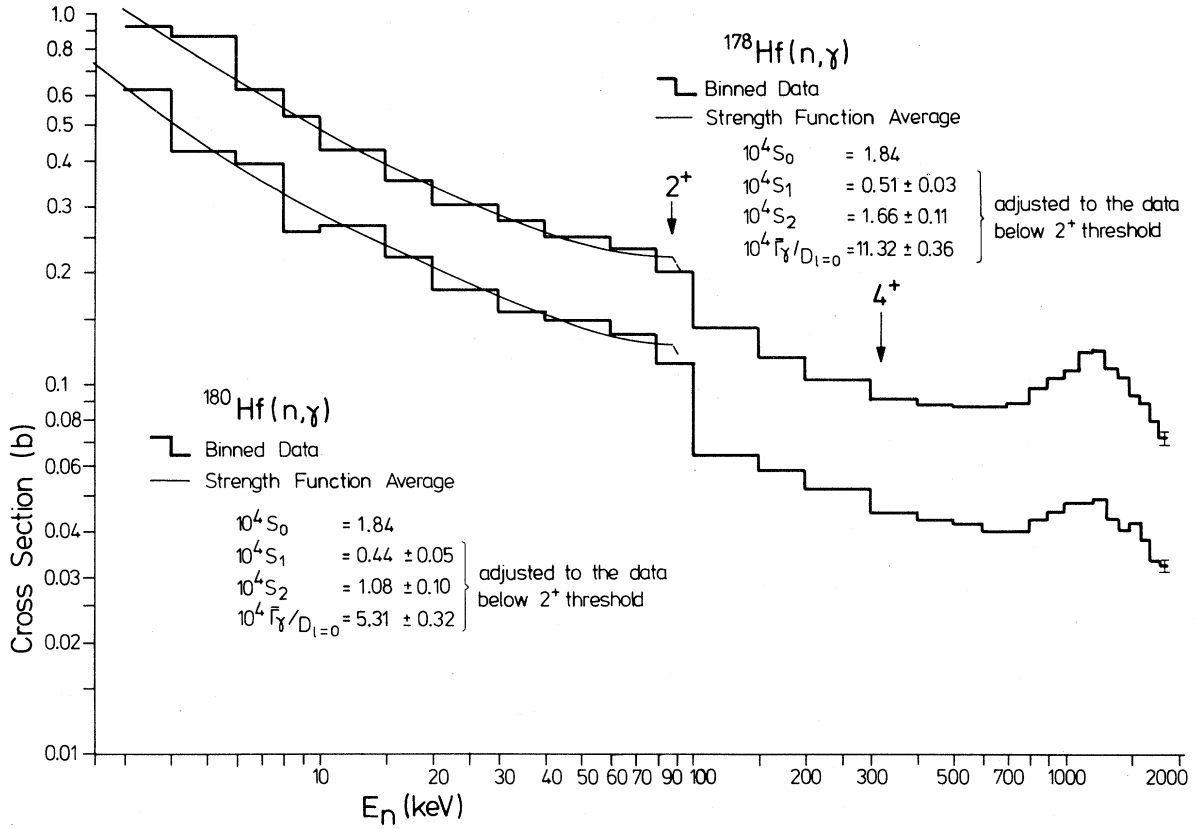

FIG. 2. Effective cross sections for ^{178,180}Hf(n,γ). The curves are a statistical model fit to the data below the inelastic threshold. The arrows mark the location of the first few excited levels. Note the pronounced effect of the opening of the first inelastic channel.

scattering plus 0.970—0.986 for self-protection, where most of the scattering was due to the oxygen in the samples. The strength function analysis was limited to the energy range below 93 keV for ^{178,180}Hf because this energy value is the threshold where the first inelastic channel opens. The competition by inelastic scattering is clearly seen in Fig. 2 by the sudden decrease of the capture cross sections. The strength function fits are indicated by the solid lines. The level density for the even isotopes was too low to allow fitting the *s*-wave strength function so the value fitted to the ^{179}Hf data was used for the even isotopes without adjustment. This is reasonable assuming a smooth and slight mass dependence as indicated by optical model calculations in the literature. The final individual strength functions of our analysis are included in Figs. 2 and 3.

In the energy region from 1 to 30 keV there are also average capture cross sections on ^{178,179,180}Hf reported by Kapchigashev.[19] The data on ^{179,180}Hf are in fair agreement with the present results; however, the ^{178}Hf cross section is about 30% higher. It is interesting to note that for the evaluation of the isotopic hafnium capture cross sections carried out by Drake *et al.*[19] the cross sections of the odd *A* isotopes of Kapchigashev were raised by about 30% in order to meet the natural hafnium capture cross section reported by Moxon.[19] With regard to our result on ^{179}Hf this artificial enlargement, at least for the ^{179}Hf capture cross section, appears to be unjustified. The present average neutron capture cross sections for ^{178,179,180}Hf are listed in Table VI.

C. Systematic uncertainties

Systematic uncertainties in the cross sections (Table VII) are dominated essentially by the saturated resonance calibration (2%) and the energy dependence of the ^{6}Li(n,α) cross section (1—3%). For the resolved resonances an additional significant uncertainty is introduced through the shape fitting procedure ($<3\%$). The resonance shape is affected by the assumptions of the resonance spin and the

TABLE VI. Histogram of the average neutron capture cross sections of ^{178,179,180}Hf.

Energy range (keV)	σ (mb) ^{178}Hf	^{179}Hf	^{180}Hf
3–4	926	3793	623
4–6	866	3049	424
6–8	620	2227	392
8–10	528	1889	259
10–15	429	1541	268
15–20	356	1267	221
20–30	306	1026	180
30–40	276	854	158
40–60	250	734	149
60–80	233	635	137
80–100	202	575	114
100–150	142	516	64
150–200	118	432	58
200–300	103	352	52
300–400	91	265	45
400–500	88	219	43
500–600	87	190	42
600–700	87	165	40
700–800	88	151	40
800–900	97	139	43
900–1000	103	126	45
1000–1100	108	116	48
1100–1200	122	105	48
1200–1300	123	101	48
1300–1400	110	86	43
1400–1500	103	83	40
1500–1600	93	83	42
1600–1700	88	81	38
1700–1800	79	67	33
1800–1900	71	66	32
1900–2000		63	

energy resolution. The independence of the primary yield from changes in the gamma-ray cascades by the pulse height weighting technique has been confirmed to 1% for various resonances: the 3.92 eV resonance in holmium, the 6.7 eV resonance in ^{238}U, and the 5.19 eV resonance in silver.[22,23] In between the runs the C_6F_6 detectors and the ^{6}Li glass detector are periodically checked by a PuBe 4.43 keV gamma ray and an ^{241}Am alpha source, respectively, to ensure that gain drifts of the electronics are negligibly small ($<0.3\%$). The neutron sensitivity of the detection system is energy dependent and varies between 10^{-3} and 10^{-4}. This correction factor is considered accurate to 30%, leading to an uncertainty of this correction smaller than 1.6%. At energies above the thresholds for inelastic scattering special attention has to be drawn to the inelastic gamma rays. Gamma rays from the 93 and 127 keV levels in ^{178,180}Hf and ^{179}Hf, respectively, lie below our bias. Contributions from higher levels can be checked by raising the bias. The high energy run (150–2000 keV) is used with a bias high enough to eliminate inelastic gamma ray response up to about 1.85 MeV. The fraction of the pulse height weighted capture spectrum above this bias was found to be 0.683, 0.729, and 0.551 (averaged in the 100–150 keV interval) for the ^{178,179,180}Hf targets, respectively. The close agreement of the high and low bias data up to 1100 keV indicates that the assumption of a constant spectrum fraction above 150 keV is warranted and that the inelastic levels are primarily depopulated by gamma cascades as expected. Other minor uncertainties can be found in Table VII.

TABLE VII. Systematic uncertainties in resonance and average capture cross section.

Saturated resonance calibration	2%
Shape of the ^{6}Li(n,α) cross section at 50 keV	1%
at 250 keV	2%
$\geq$500 keV	3%
Pulse height weighting technique	1%
Neutron sensitivity of detection systen (Sample scattered neutrons)	$<$1.6%
γ-ray self absorption of sample	0.4%
Multiple scattering self-protection	0.5%
Detector bias extrapolation ($E_{bias}=153$ keV)	0.4%
Misalignment of sample or neutron beam	$<$0.2%
Uncertainty in detector efficiency by gain Drifts of electronics	$<$0.4%[a]
Resonance shape (unknown spin, resolution function)	$<$3%

[a]1.9% for the ^{179}Hf measured during a time when the gain of one detector decreased significantly and probably not uniformly.

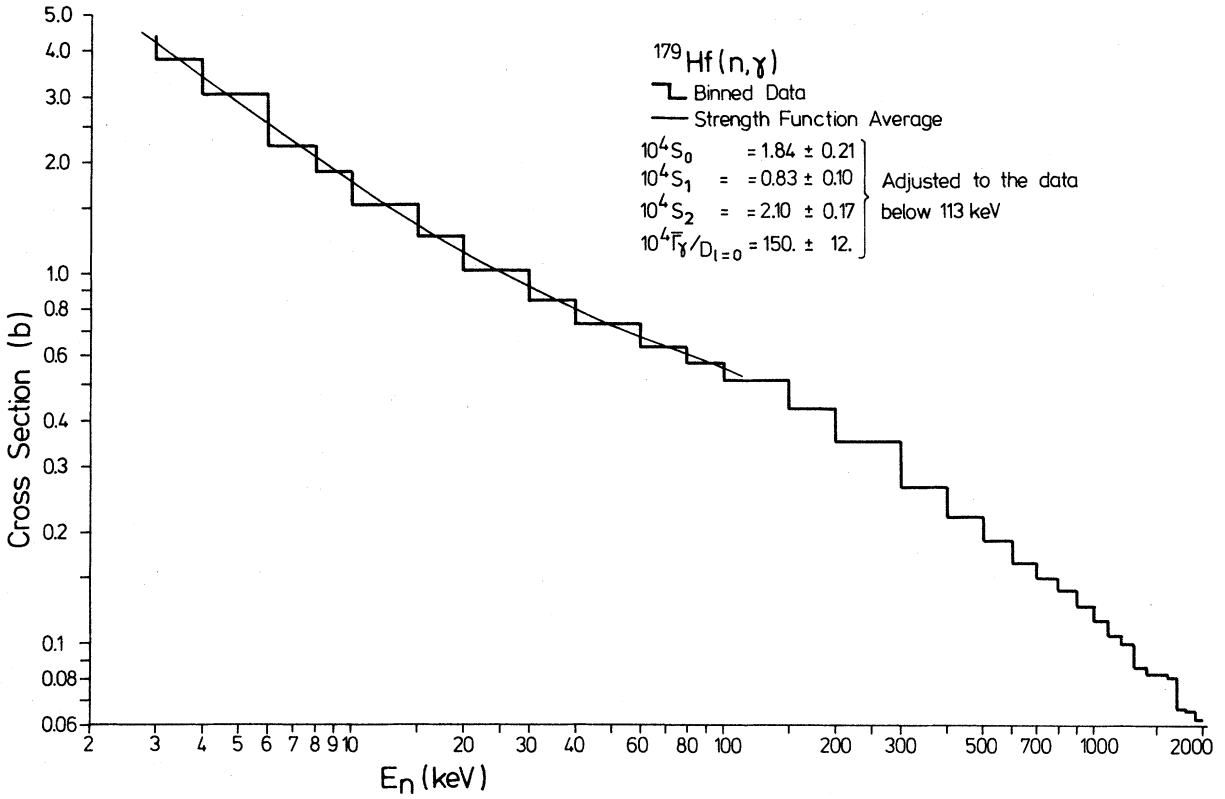

FIG. 3. Effective cross section for ^{179}Hf(n,γ). The curve is a statistical model fit to the data below the inelastic threshold.

D. Maxwellian average capture cross sections of ^{178,179,180}Hf and their solar *r*-process abundances

Maxwellian averaged capture cross sections $\langle\sigma v\rangle/v_T$ were computed from the differential data for temperatures kT between 5 and 100 keV by numerical integration according to the following formula:

$$\frac{\langle\sigma v\rangle}{v_T}=\frac{2}{\sqrt{\pi}}\int_0^\infty \sigma(E)Ee^{-E/kT}dE \Big/ \int_0^\infty Ee^{-E/kT}dE \ .$$

In practice it is sufficient to carry out the integration over the limited energy interval below 500 keV for the present $\langle\sigma v\rangle/v_T$ values without essential error. The cross section below 2.6 keV was approximated by using the strength functions. The results are listed in Table VIII. The $\langle\sigma v\rangle/v_T$ values at $kT=30$ keV, which in the following discussion will be simply given as $\underline{\sigma}$ in italics, can yield improved *r*-process abundances for ^{178,179,180}Hf by subtracting the *s*-process contribution as described in the recent $\underline{\sigma}N_s$ systematics report by Käppeler *et al.*[24]

$$N_r(^A\mathrm{Z})=N_\odot(^A\mathrm{Z})-\underline{\sigma}N_s(^A\mathrm{Z})/\underline{\sigma}(^A\mathrm{Z}) \ ,$$

where N_r and $N_\odot$ (Ref. 25) are the *r* process and solar abundances of a nucleus with mass number A and proton number Z and $\underline{\sigma}N_s$ is the Maxwellian averaged capture cross section times *s*-process abundance taken from Ref. 24. The N_r values calculated are included in Table VIII. The Maxwellian averaged capture cross section for $kT=25$ keV is in excellent agreement with the result $\underline{\sigma}=189\pm10$ mb from a previous measurement reported by Beer *et al.*[26]

This is reassuring, as the measurements were carried out with totally different techniques: The previous measurement[26] made use of the activation method; the present measurement used the time-of-flight technique and the prompt emitted gamma rays to detect the capture events. The agreement of the ^{180}Hf results also represents a crucial check. The activation measurement[11,26] with natural Hf yielded at the same time $\underline{\sigma}(^{179}\mathrm{Hf}\xrightarrow{n,\gamma}{}^{180}\mathrm{Hf}^m)$, and this

TABLE VIII. Maxwellian averaged capture cross sections and *r*-process abundances. For the cross sections an overall uncertainty of 3% is estimated.

Thermal energy kT (keV)	σ (mb) ^{178}Hf	^{179}Hf	^{180}Hf	N_r[a] (Si≡10^6) ^{178}Hf	^{179}Hf	^{180}Hf
5	842	2990	478			
6	743	2635	424			
7	671	2371	386			
8	616	2168	356			
9	573	2006	332			
10	538	1874	313			
12.5	475	1627	277			
15	432	1457	253			
17.5	400	1330	234			
20	375	1233	219			
25	338	1091	196			
30	310	991	179	0.0278	0.0177	0.0290
35	288	917	165			
40	270	858	153			
45	254	810	143			
50	241	769	134			
60	220	704	121			
70	203	652	110			
85	184	591	98			
100	170	543	89			

[a] $N_r = N_\odot - \underline{\sigma} N_s / \underline{\sigma}$. The calculation was performed using the solar abundances $N_\odot$ from Cameron and the $\underline{\sigma} N_s$ values from Käppeler *et al.* (Ref. 23).

partial cross section is used in this work to calculate the isomeric population probability of ^{180}Hf^m for the *s*-process analysis of the ^{180}Ta^m abundance.

VI. THE ^{180}Ta^m CAPTURE CROSS SECTION

The 30 keV neutron capture cross section of ^{180}Ta^m is introduced into the study of an *s*-process origin of this nucleus as a consequence of the supposed *s*-process flow. As the presently available amount of ^{180}Ta^m (155 mg enriched in ^{180}Ta^m to 5.47%) is not sufficient for a neutron capture cross section measurement, we have to rely on an estimate via a statistical model calculation. The formalism used for this purpose is the same as described in Refs. 27 and 28. The cross section $\sigma_{J,l}$ for neutrons of angular momentum l captured by levels of total angular momentum J is written as

$$\sigma_{Jl} = \frac{2\pi^2}{k^2} g_J \sum_j \frac{\overline{\Gamma_{n,J}(l,j)}\,\overline{\Gamma_{\gamma,J}}}{\bar{D}_J \bar{\Gamma}_J} F \ ,$$

where k is the wave number of the incident neutron, g_J the statistical spin factor, $\Gamma_{n,J}(l,j)$ the neutron width for channel spin j, $\Gamma_{\gamma,J}$ the radiation width, Γ_J the total width, and D_J the level spacing. The

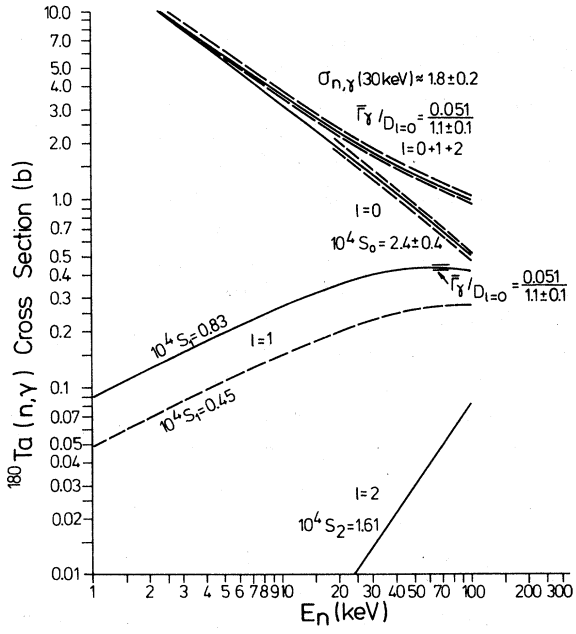

FIG. 4. The average cross section of ^{180}Ta as a function of energy calculated with the statistical model. The various contributions from *s*, *p*, and *d* waves are shown separately. The uncertainties are indicated by dashed lines.

width fluctuation factor F is identical to the respective quantity S defined in Ref. 27. For the calculation of the $^{180}Ta^m$ cross section J-independent s-, p-, and d-wave neutron strength functions S_l were introduced in the conventional way. Further assumptions were (1) $\bar{\Gamma}_{\gamma,J}$ and $\bar{D}_J$ are energy independent and (2) $\bar{\Gamma}_{\gamma,J}=\bar{\Gamma}_\gamma$ and $\bar{D}_J=\bar{D}/(2J+1)$.

For the s-wave strength function $S_{l=0}$, the average radiation width $\bar{\Gamma}_\gamma$, and the average level spacing $\bar{D}$, the values of Harvey *et al.*[29] were taken which are derived from a transmission experiment in the energy range 0.3 to 300 eV. The quoted values are the following: $S_{l=0}=(2.4\pm0.4)\times10^{-4}$, $\bar{\Gamma}_\gamma=51\pm1$ meV, and $\bar{D}=1.1\pm0.1$ eV.

The p- and d-wave strength functions were estimated using the systematic behavior of the neighboring nuclei Hf and W. Figure 4 shows the present analysis. The individual contributions from s-, p-, and d-wave capture are plotted together with the sum. For the p-wave contribution a lower limit is also indicated. A 30 keV $^{180}Ta^m$ capture cross section of 1800 ± 200 mb is derived. The quoted uncertainty mainly reflects the uncertainty in the level density.

VII. s- AND POST r-PROCESS NUCLEOSYNTHESIS OF ^{180}Ta

The present capture cross-section measurements on ^{179,180}Hf have a straightforward bearing on the possible neutron capture nucleosynthesis of nature's rarest stable isotope $^{180}Ta^m$ (actually an isomeric state). This mechanism of nucleosynthesis was suggested recently by Beer and Ward.[11] As was demonstrated in Ref. 11, the key to a neutron capture production is a small β-decay branching of an isomeric state in ^{180}Hf at 1.14 MeV with a total half-life of 5.5 h. Any s- or post-r-process production of $^{180}Ta^m$ depends on the possibilities of populating this isomeric level in ^{180}Hf. The population by s-process nucleosynthesis is attained by neutron capture on ^{179}Hf. The population via post-r-process nucleosynthesis must be conducted by a branch in the ^{180}Lu β decay to $^{180}Hf^m$. According to Ref. 11 one can write for the s-process abundance of $^{180}Ta^m$ $N_s(^{180}Ta^m)$ and the respective r-process abundance $N_r(^{180}Ta_m)$

$$N_s(^{180}Ta^m)=\frac{\underline{\sigma}^m(^{179}Hf)}{\underline{\sigma}(^{179}Hf)}f^m_{\beta^-}\frac{\underline{\sigma}N_s(A=180)}{\underline{\sigma}(^{180}Ta^m)}\,, \tag{1}$$

$$N_r(^{180}Ta^m)=f^{180}_m f^m_{\beta^-}\left[N_\odot(^{180}Hf)-\frac{\underline{\sigma}N_s(A=180)}{\underline{\sigma}(^{180}Hf)}\right], \tag{2}$$

where $\underline{\sigma}$ designates Maxwellian averaged capture cross sections of the indicated isotopes and $\underline{\sigma}^m(^{179}Hf)$ stands for the partial capture cross section of ^{179}Hf to the $^{180}Hf^m$ isomer. This quantity was measured for $kT=25$ keV by Beer and Ward[11] as 13.5 ± 0.6 mb. $\underline{\sigma}N_s(A=180)$ is the neutron capture times s-process abundance value at mass number 180 which amounts to 5.53 (mb$\times$Si$\equiv10^6$) according to the recent systematic calculation of Käppeler *et al.*[24] $N_\odot(^{180}Hf)=0.0599$ (Ref. 25) represents the solar abundance of ^{180}Hf. $f^m_{\beta^-}$ and f^{180}_m are the still undetermined branching factors for the transitions

$$^{180}Hf^m \xrightarrow{\beta^-} {}^{180}Ta^m$$

and

$$^{180}Lu \xrightarrow{\beta^- \text{ or } \beta^-+\gamma} {}^{180}Hf^m\,,$$

respectively.

Owing to the present measurements two important quantities, the population probability

$$\underline{\sigma}^m(^{179}Hf)/\underline{\sigma}(^{179}Hf)=(1.24\pm0.06)\,\%$$

[Eq. (1)] and the r-process abundance

$$N_r(^{180}Hf)=[N_\odot(^{180}Hf)-\underline{\sigma}N_s(A=180)/\underline{\sigma}(^{180}Hf)]=0.0285\ (Si\equiv10^6)$$

[Eq. (2)] are experimentally verified. In addition, $\underline{\sigma}(^{180}Ta^m)$ could be calculated on the basis of experimental information on level density, strength functions, and average radiation width. Therefore, the final size of the s- and r-process abundance contributions depends on the determination of $f^m_{\beta^-}$ and f^{180}_m. $f^m_{\beta^-}$ was estimated to $0.14\%\le f^m_{\beta^-}\le22\%$ because the β decay is an allowed Gamow-Teller transition. An upper limit $f^m_{\beta^-}\le3.8\%$ was given by Gallagher *et al.*[30] based on a measurement of the $^{180}Hf^m$ β spectrum.

In the frame of the Nilsson model, the $^{180}Hf^m$ isomer is characterized as a relatively pure two proton state with a configuration $K^\pi=8^-$ ($\frac{7}{2}^+[404]_p$, $\frac{9}{2}^-[514]_p$) (Ref. 31) and the measurement of spin and magnetic dipole moment of $^{180}Ta^m$ is best

reproduced for a parallel coupling of a $\frac{9}{2}^-[514]$ proton and a $\frac{9}{2}^+[624]$ neutron configuration. Therefore, the β^- transition $^{180}\mathrm{Hf}^m \xrightarrow{\beta^-} {}^{180}\mathrm{Ta}^m$ can be characterized by the transformation $\frac{9}{2}^+[624]_n \rightarrow \frac{7}{2}^+[404]_p$ indicating an allowed hindered β^- transition which consistently is observed with a logft value of 6 to 8 (Ref. 32).

The presently described β^- transition in $^{180}\mathrm{Hf}^m$ to $^{180}\mathrm{Ta}^m$ has its exact counterpart in the $^{182}\mathrm{Hf}^m(J^\pi=8^-) \rightarrow {}^{182}\mathrm{Ta}(J^\pi=9^-)$ investigated by Ward *et al.*[33] These authors determined for this transition a logft value of 6.4 which should also represent a good estimate for our $^{180}\mathrm{Hf}^m \rightarrow {}^{180}\mathrm{Ta}^m\beta^-$ decay. Using the tabulated f values of Gove *et al.*[34] we obtain a β^- decay half-life of $T_{1/2}=67.4$ d.

Before we proceed to calculate the branching factor $f^m_{\beta^-}$ we must bear in mind that the $^{180}\mathrm{Hf}^m$ nuclei are highly ionized under s-process conditions. Even the K shell is almost completely empty. This gives rise to the following effects which act to increase the branching factor $f^m_{\beta^-}$:

(1) The 5.5 h $^{180}\mathrm{Hf}^m$ decay via the 57.5 and 500.7 keV transitions is delayed because the conversion is hindered. The individual effective half-lives are $(1/b)(1+\sum\alpha_i)5.5$ h where the α's are the various conversion coefficients and b the branching factor.

(2) The $^{180}\mathrm{Hf}^m \rightarrow {}^{180}\mathrm{Ta}^m\beta$ decay is increased by bound state β decay $\lambda_{\beta B}$

$$\lambda_{\beta\mathrm{eff}}=\lambda_{\beta C}(1+\lambda_{\beta B}/\lambda_{\beta C}) .$$

For the continuum β decay rate $\lambda_{\beta C}$ the laboratory half-life can be used.

The first effect leads to a total isomeric half-life of 7.75 h. This increased half-life is mainly due to the hindered L shell conversion of the 57.5 keV transition (K conversion is energetically not possible).

The second effect, bound state β decay treated according to the formulas developed by Bahcall,[35] yielded $\lambda_{\beta B}/\lambda_{\beta C}=0.5$. Therefore our effective β half-life becomes $67.4/1.5=45$ d and $f^m_{\beta^-}$ is including all effects

$$f^m_{\beta^-} \cong 0.7\% .$$

We can now estimate the s-process abundance of $^{180}\mathrm{Ta}^m$ to be $N_s(^{180}\mathrm{Ta}^m) \cong 2.6\times10^{-7}$ (Si$\equiv10^6$); this is only 11% of the $^{180}\mathrm{Ta}^m$ solar abundance.

In principle similar effects are to be expected for $f^m_{\beta^-}$ in the post r-process environment. But for an estimate of the unknown factor f^{180}_m we will simply assume $f^m_{\beta^-}=0.34\%$ calculated from the laboratory half-lives.

In order to reproduce the $^{180}\mathrm{Ta}^m$ solar abundance totally by the r-process $f^{180}_m \leq 2.5\%$ is required. Unfortunately, the transitions of the ^{180}Lu decay are not better established than 6% so that it cannot be decided if an intensity feeding of the 8^- isomer of the same magnitude is possible.[36] There are, for instance, discrepancies between the γ intensities and energies of the $(3^-,6^-)^{180}$Hf level at 1607.7 keV from the 90.2% ^{180}Lu β decay and the respective intensitites and energies from the $^{179}\mathrm{Hf}(n,\gamma)$ reaction. In addition, due to the work of Takahashi *et al.*[37] the existence of a $^{180}\mathrm{Lu}^m$ high spin isomer is indicated which could directly feed the $^{180}\mathrm{Hf}^m$ isomeric state. The result of Takahashi *et al.*[37] was, however, not reproduced by the measurement of Swindle *et al.*[38]

VIII. CONCLUSIONS

In this work the origin of $^{180}\mathrm{Ta}^m$ by neutron capture nucleosynthesis was investigated. The quantitative analysis showed that the s process can contribute to the buildup of the $^{180}\mathrm{Ta}^m$ solar abundance only insignificantly provided our estimated logft value of 6.4 for the $^{180}\mathrm{Hf}^m \rightarrow {}^{180}\mathrm{Ta}^m$ beta transition is correct. A final clarification must await a measurement of the branching factor $f^m_{\beta^-}$. If it should turn out that $f^m_{\beta^-}$ is substantially greater than the present estimate one has to investigate the question of how the $^{180}\mathrm{Ta}^m$ isomer could survive in the hot stellar photon bath under s-process temperature conditions because any excited level which could equilibrate the isomer with the 8.1 h ground state would rapidly destroy the result of the s-process synthesis. This would mean that $^{180}\mathrm{Ta}^m$ can be used as a *stellar thermometer* of the s process.

There is still the possibility that post-r-process nucleosynthesis can produce a sizable amount of $^{180}\mathrm{Ta}^m$. To confirm this would mainly require a careful search for a branch in the ^{180}Lu decay feeding the $^{180}\mathrm{Hf}^m$ isomeric state. For this kind of nucleosynthesis again one has to clarify how an isomeric state (the only known quasistable isomer) can survive in the hot post supernova stage of a star. The analysis of this problem might yield constraints about the *temperature conditions* of a supernova shortly after the explosion. The study of these extended questions in the frame of s- and r-process nucleosynthesis requires, however, a detailed knowledge of the ^{180}Ta level scheme below 500 keV.

ACKNOWLEDGMENTS

One of the authors (H.B.) expresses his appreciation to the U.S. Department of Energy for funding a stay at ORNL during which part of this work was done. Oak Ridge National Laboratory is operated by Union Carbide Corporation under contract W-7405-eng-26 with the U.S. Department of Energy.

[1]J. Audouze, Astron. Astrophys. 8, 436 (1970).
[2]H. Mabuchi and A. Masuda, Nature (London) 226, 338 (1970).
[3]K. L. Hainebach, D. N. Schramm, and J. B. Blake, Astrophys. J. 205, 920 (1976).
[4]T. G. Harrison, Astrophys. Lett. 17, 61 (1976); 18, 7 (1976).
[5]H. Beer and F. Käppeler, Phys. Rev. C 21, 534 (1980).
[6]H. Beer, F. Käppeler, K. Wisshak, and R. A. Ward, Astropyhs. J. Suppl. Ser. 46, 295 (1981).
[7]F. A. White, T. L. Collins, and F. M. Rourke, Phys. Rev. 98, 1174 (1955).
[8]B. Burghardt, R. Harzer, H. J. Hoeffgen, and G. Meisel, Phys. Lett. 92B, 64 (1980).
[9]K. S. Sharma, R. J. Ellis, V. P. Derenchuk, R. C. Barber, and H. E. Duckworth, Phys. Lett. 91B, 211 (1980).
[10]E. B. Norman, private communication.
[11]H. Beer and R. A. Ward, Nature (London) 291, 308 (1981).
[12]R. L. Macklin *et al.*, Phys. Rev. C (to be published).
[13]R. L. Macklin, N. W. Hill, and B. J. Allen, Nucl. Instrum. Methods 96, 509 (1971).
[14]H. Maier-Leibnitz, private communication .
[15]R. L. Macklin, J. Halperin, and R. R. Winters, Nucl. Instrum. Methods 164, 213 (1979).
[16]B. J. Allen, R. L. Macklin, R. R. Winters, and C. Y. Fu, Phys. Rev. C 8, 1504 (1973).
[17]R. L. Macklin and B. J. Allen, Nucl. Instrum. Methods 91, 565 (1971).
[18]R. L. Macklin, Nucl. Instrum. Methods 59, 12 (1976).
[19]M. K. Drake, D. A. Sargis, and T. Maung, report EPRI, NP-250, 1976, containing unpublished data from S. P. Kapchigashev and M. C. Moxon.
[20]R. L. Macklin, Nucl. Instrum. Methods 26, 213 (1964).
[21]L. Dresner, Nucl. Instrum. Methods 16, 176 (1962).
[22]R. L. Macklin, J. Halperin, and R. R. Winters, Phys. Rev. C 11, 1270 (1975).
[23]N. Yamamuro, T. Hayase, T. Doi, Y. Fujita, K. Kobayashi, and R. C. Block, Nucl. Instrum. Methods 133, 531 (1976).
[24]F. Käppeler, H. Beer, K. Wisshak, D. D. Clayton, R. L. Macklin, and R. A. Ward, Astrophys. J. 257, 821 (1982).
[25]A. G. W. Cameron, in *Nuclear Astrophysics,* edited by C. A. Barnes, D. D. Clayton, and D. N. Schramm (Cambridge University, Cambridge, England, 1981).
[26]H. Beer, F. Käppeler, K. Wisshak, Astron. Astrophys. 105, 270 (1982).
[27]A. M. Lane and J. E. Lynn, Proc. Phys. Soc., London, Sect. A 70, 557 (1957).
[28]J. H. Gibbons, R. L. Macklin, P. D. Miller, and J. H. Neiler, Phys. Rev. 122, 182 (1961).
[29]J. A. Harvey, N. W. Hill, and E. R. Mapoles Oak Ridge National Laboratory Report No. 5025, 1975 (unpublished).
[30]C. J. Gallagher, Jr., M. Jørgensen, and O. Skilbreid, Nucl. Phys. 33, 285 (1962).
[31]H. J. Körner, F. E. Wagner, and B. D. Dunlap, Phys. Rev. Lett. 27, 1593 (1971).
[32]M. A. Preston, *Physics of the Nucleus* (Addison-Wesley, Reading, Mass., 1963), p. 451.
[33]T. E. Ward, P. E. Haustein, J. B. Cumming, and Y. Y. Chu, Phys. Rev. C 10, 1983 (1974).
[34]N. B. Gove, and M. J. Martin, Nucl. Data Tables 10, 205 (1971).
[35]J. N. Bahcall, Phys. Rev. 124, 495 (1961).
[36]L. R. Greenwood, Nucl. Data Sheets 15, 559 (1975).
[37]K. Takahashi, T. Kuroyanagi, H. Yuta, K. Kotajima, K. Nagatani, and H. Morinaga, J. Phys. Soc. Jpn. 16, 1664 (1961).
[38]D. L. Swindle, T. E. Ward, and P. K. Kuroda, Phys. Rev. C 3, 259 (1971).